




ORIGINAL ARTICLE

Antitumor effects of novel mAbs against cationic amino acid transporter 1 (CAT1) on human CRC with amplified CAT1 gene

Kouki Okita^{1,2} | Yuta Hara¹ | Hiroshi Okura¹ | Hidemi Hayashi³ | Yoko Sasaki¹ | Sachiko Masuko^{1,3} | Eri Kitadai³ | Kazue Masuko¹ | Soshi Yoshimoto^{1,4} | Natsumi Hayashi^{1,4} | Reiko Sugiura⁴  | Yuichi Endo⁵ | Shogo Okazaki⁶ | Sayaka Arai⁷ | Toshiaki Yoshioka⁷ | Toshiharu Matsumoto⁸ | Yasutaka Makino⁹ | Hiromitsu Komiyama⁹  | Kazuhiro Sakamoto⁹ | Takashi Masuko^{1,5*} 

¹Cell Biology Laboratory, School of Pharmacy, Kindai University, Osaka, Japan

²Production and Manufacturing, Carna Biosciences, Inc., Kobe, Japan

³Division of Gene Regulation, Institute for Advanced Medical Research, School of Medicine, Keio University, Tokyo, Japan

⁴Laboratory of Molecular Pharmacogenomics, Faculty of Pharmacy, Kindai University, Osaka, Japan

⁵Natural Drug Resources, Faculty of Pharmacy, Kindai University, Osaka, Japan

⁶Division of Cell Fate Regulation, Research Institute for Biomedical Sciences, Tokyo University of Science, Chiba, Japan

⁷Field of Basic Science, Department of Occupational therapy, Graduate School of Health Sciences, Akita University, Akita, Japan

⁸Department of Diagnostic Pathology, Faculty of Medicine, Juntendo University, Tokyo, Japan

⁹Department of Coloproctological Surgery, Faculty of Medicine, Juntendo University, Tokyo, Japan

Correspondence

Takashi Masuko, Natural Drug Resources, Faculty of Pharmacy, Kindai University, 3-4-1 Kowakae, Higashiosaka-shi, Osaka 577-8502, Japan.

Email: masuko@phar.kindai.ac.jp

Abstract

Copy number alterations detected by comparative genomic hybridization (CGH) can lead to the identification of novel cancer-related genes. We analyzed chromosomal aberrations in a set of 100 human primary colorectal cancers (CRCs) using CGH and found a solute carrier (SLC) 7A1 gene, which encodes cationic amino acid transporter 1 (CAT1) with 14 putative transmembrane domains, in a chromosome region (13q12.3) with a high frequency of gene amplifications. SLC7A1/CAT1 is a transporter responsible for the uptake of cationic amino acids (arginine, lysine, and ornithine) essential for cellular growth. Microarray and PCR analyses have revealed that mRNA transcribed from CAT1 is overexpressed in more than 70% of human CRC samples, and RNA interference-mediated knockdown of CAT1 inhibited the cell growth of CRCs. Rats were immunized with rat hepatoma cells expressing CAT1 tagged with green fluorescent protein (GFP), and rat splenocytes were fused with mouse myeloma cells. Five rat monoclonal antibodies (mAbs) (CA1 ~ CA5) reacting with HEK293 cells expressing CAT1-GFP in a GFP expression-dependent manner were selected from established hybridoma clones. Novel anti-CAT1 mAbs selectively reacted with human CRC tumor tissues compared with adjacent normal tissues according to immuno-histochemical staining and bound strongly to numerous human cancer cell lines by flow cytometry. Anti-CAT1 mAbs exhibited internalization activity, antibody-dependent cellular cytotoxicity, and migration inhibition activity against CRC cell lines. Furthermore, CA2 inhibited the in vivo growth of human HT29 and SW-C4 CRC tumors in nude mice. This study suggested CAT1 to be a promising target for mAb therapy against CRCs.

Kouki Okita and Yuta Hara contributed equally to this work.

[†]This laboratory was closed at the end of March (2020), after the mandatory retirement of Takashi Masuko.

This is an open access article under the terms of the Creative Commons Attribution-NonCommercial-NoDerivs License, which permits use and distribution in any medium, provided the original work is properly cited, the use is non-commercial and no modifications or adaptations are made.

© 2020 The Authors. *Cancer Science* published by John Wiley & Sons Australia, Ltd on behalf of Japanese Cancer Association.

Funding information

Strategic Research Foundation at Private Universities, Grant/Award Number: S1411037; Japan Society for the Promotion of Science, Grant/Award Number: 16K10476

KEYWORDS

CAT1, CRC, mAb, oncogene addiction, SLC7A1

1 | INTRODUCTION

Cancer cells have common properties such as unlimited proliferation, self-sufficiency in growth signals, and resistance to apoptosis. Activation of oncogenes by genomic aberrations is a major pathogenic mechanism in many cancers.¹⁻³ Gene amplification is responsible for the initiation and progression of many solid tumors, including colorectal cancers (CRCs).

Cancer cells can also be highly dependent on the activity of a single oncogene for the maintenance of the malignant phenotype and cell survival, and this phenomenon is known as oncogene addiction.^{4,5} Clinically relevant evidence for the concept of oncogene addiction comes from examples of the therapeutic efficacy of monoclonal antibodies (mAbs) or low-molecular weight compounds, which inhibit specific oncogene products. Examples include gefitinib, erlotinib, and lapatinib, which target oncogenic human epidermal growth factor receptor (HER)1/EGFR in non-small cell lung cancers, and trastuzumab and pertuzumab recognizing HER2 in breast cancers.⁶⁻⁸ Subsequent studies demonstrated that cetuximab and panitumumab targeting HER1 may have significant antitumor activity against head and neck cancers and CRCs.⁹ These studies on HER1 and HER2 also provided insights into the concept of oncogene addiction, especially for oncogenes activated by a mechanism of gene amplification. Cancer cells may be much more dependent on the activity of a specific oncogene than normal cells because a given target gene activated by gene amplification leads to sustained overexpression of relevant proteins in cancer cells compared with normal cells.¹⁰

In this context, we used a combination of array-based comparative genomic hybridization (CGH) and quantitative polymerase chain reaction (qPCR) to seek for highly expressed genes that are associated with gene amplification in CRCs. Solute carrier (SLC)7A1-coding cationic amino acid (AA) transporter (CAT1) was identified as an overexpressed gene mapped to 13q12. SLC7A1/CAT1 is a transporter responsible for the uptake of cationic AA (arginine, lysine, and ornithine) essential for cellular growth.

In this study, we have produced novel mAbs recognizing the extracellular domain of CAT1 and demonstrated higher expression of CAT1 proteins in many CRC cell lines and surgically removed CRC specimens. Furthermore, internalization of CAT1, antibody-dependent cellular cytotoxicity (ADCC), inhibition of CRC migration, and in vivo antitumor effects of anti-CAT1 mAb on xenografted CRC cells in nude mice were demonstrated.

2 | MATERIALS AND METHODS

2.1 | Clinical specimens

One hundred CRC frozen tissue samples from surgical specimens were obtained from Juntendo University, Tokyo, Japan. The experimental protocol (No. 2 013 145) was approved by the institutional review board. Specimens were collected for 8 years from 2004 through 2011. All patients provided informed consent prior to enrollment. Normal and cancer cells were collected from specimens of patients for genomic DNA and RNA extraction. From frozen sections (16 μ m thick), normal (distant from cancer) and cancer (>95% tumor cells) regions were manually micro-dissected, under the guidance of two skillful pathologist.

2.2 | Genomic DNA sample preparation

Genomic DNA was extracted using the Quick Gene SP-kit DNA tissue (Wako Pure Chemical Industries), and quality was characterized by agarose gel electrophoresis. Human Male Genomic DNA or Human Female Genomic DNA (Merck-Millipore) was used for sex-matched normal reference DNA.

2.3 | Preparation of whole-genome DNA microarray

The DNA microarray was created with complete coverage of the human genome using 12 310 individually amplified bacterial artificial chromosomes (BAC) clones. All BAC clones were cultured from a single colony and confirmed by PCR amplification using clone-specific primers that were designed in-house. Extracted BAC DNA was digested with BstYI and amplified by ligation-mediated PCR. The products were printed on glass slides with an inkjet-type spotter.

2.4 | Analysis of genome copy number: Array CGH analysis

Alu I- and Rsa I-digested genomic DNAs were labeled by random priming with Alexa555-dCTP (test DNA) and Alexa647-dCTP (reference DNA) using the BioPrime Plus Array CGH Indirect Genomic Labeling System (Invitrogen). Labeled test and reference DNA was ethanol-precipitated in the presence of Cot-1 DNA, redissolved

in a hybridization mix, and denatured at 70°C for 10 minutes. After incubation at 42°C for 5 minutes, the mixture was applied to the whole-genome DNA microarray (LinkGenomics) covered with an MAUI Mixer hybridization chamber (BioMicro Systems). After incubation at 42°C for 48 hours, slides were washed with $2 \times \text{SSC}/0.1\% \text{SDS}$ buffer and $0.1 \times \text{SSC}/0.1\% \text{SDS}$ buffer for five times. After rinsing with $0.01 \times \text{SSC}$ buffer and air-drying, slides were scanned by a Microarray Scanner (Agilent Technologies) and analyzed using Gene-Pix Pro 4.0 imaging software (Axon Instruments). Thresholds for gains and losses were set to 1.2 and 0.8, respectively.

2.5 | Analysis of mRNA expression: microarray analysis

RNA samples were labeled using the Low Input Quick Amp Labeling kit (Agilent Technologies). Labeled cRNA was hybridized to an oligo-nucleotide microarray (Whole Human Genome $4 \times 44\text{K}$, Agilent Technologies) at 60°C for 17 hours. After washing with the Gene Expression Wash Buffer kit (Agilent Technologies) and drying, the slides were scanned by an Agilent Microarray Scanner and analyzed with the Feature Extraction software (Agilent Technologies). Normalization was performed using global normalization methods.

2.6 | Reverse transcription quantitative PCR analysis (RT-qPCR)

Total RNA was extracted using the RNeasy micro kit (Qiagen), and quality was assessed using BioAnalyzer (Agilent Technologies). RT was performed using the SuperScript III First-Strand synthesis system for qRT-PCR (Invitrogen). Synthesized cDNA was stored at -80°C until use. Real-time RT-qPCR was performed with 25 ng of cDNA using *SLC7A1*-specific primers, Power SYBR Green PCR Master Mix (Applied Biosystems), and the Applied Biosystems 7500 Real-time PCR system under the reaction condition of 95°C for 10 minutes, followed by 40 cycles of heat denaturation at 95°C for 15 seconds and annealing/elongation at 60°C for 1 minutes. Normalization was performed with TATA-binding protein as an internal control.

2.7 | RNA interference-mediated knockdown (KD)

Small interfering RNAs (siRNAs) for the candidate transcript of *SLC7A1* and negative control siRNA were purchased from Dharmacon. Transfections with Lipofectamine RNAiMAX (Invitrogen) were performed according to the manufacturer's protocol. For the KD of *SLC7A1*, 1.5×10^4 cells were plated in each well of six-well plates (Corning Japan), to which siRNA-Lipofectamine complexes were immediately added, resulting in a final

RNA concentration of 10 nmol/L. After 48 hours, mRNA levels were measured by RT-qPCR and cells were subcultured into each well of 96-well plates.

2.8 | Cell culture

RH7777 rat hepatoma cells were kindly donated by Dr Chiba K (Mitsubishi Tanabe Pharma). Human CRC cell lines (Caco2, COLO 201, COLO 205, COLO 320DM, HCT116, HT29, LS1034, LS123, LS174T, LS180, RKO, RKO-E6, SNU-C1, SW1116, WiDr), PK-1, PK-59, PANC-1, MIA PaCa-2 pancreatic, BT20, BT474 breast, A549, NCI-H2170 lung cancers, and P3U1 mouse myeloma cells were purchased from the American Type Culture Collection (ATCC). CCK-81 and OUMS23 human CRC cells were purchased from JCRN Cell Bank. SW-C4 is a clone originating from SW1116, and LS-LM4¹¹ is a highly liver-metastatic clone from LS174T. The HEK293F human embryonic kidney cell line was purchased from Invitrogen. All cells were cultured in RD medium,¹² which is a blended medium of equivalent volumes of RPMI-1640 and Dulbecco's modified Eagle medium (Nissui Pharmaceutical Co, Ltd) containing 7% heat-inactivated fetal bovine serum (FBS, Thermo Fisher Scientific Inc) at 37°C under humid conditions. Aseptic processing during cell culture was ideally controlled by a MediAir air purifier (Pieras Co., Ltd) equipped in the cell-culture room. Cell growth was measured as previously described.¹³ Briefly, a WST-8-based cell counting kit (Dojin Chemicals) was used, and 450 nm was measured using a microplate reader.

2.9 | Animals

All animals were purchased from SLC Inc and housed in specific pathogen-free conditions. They were kept individually in plastic cages under a standard light/dark cycle (12-hour light cycle starting at 7:00) at a constant temperature of $23 \pm 1^\circ\text{C}$, and had ad libitum access to food and water. All animal experiments in the present study were approved by the Committee for the Care and Use of Laboratory Animals at Kindai University (KAPS-23-004 and KAPS-27-006) and performed following the institutional guidelines.

2.10 | Flow cytometry (FCM)

Cells ($1-3 \times 10^5$ cells) were incubated with the primary mAbs (10 $\mu\text{g}/\text{mL}$) on ice for 1 hour. Following two washes with PBS containing 0.2% bovine serum albumin (BSA, Wako Pure Chemical)-phosphate buffered saline (PBS), cells were incubated with phycoerythrin (PE)-conjugated donkey anti-rat IgG (H + L) secondary polyclonal antibody (pAb) (Jackson ImmunoResearch) diluted 1:300 in 1% BSA-PBS on ice for 45 minutes. Following three washes with 0.2% BSA-PBS, the fluorescence intensity of

individual cells was analyzed using FACS Calibur and LSR-Fortessa flow cytometers (Becton-Dickinson). Using the values of the mean fluorescence intensity (MFI) with or without the primary mAbs, the subtracted (Δ) MFI was calculated.

2.11 | Establishment of anti-human CAT1 hybridomas

Transfectants and mAbs were generated as previously noted.^{14,15} Human CAT1 cDNA was obtained by RT of total RNA isolated from HT29 cells using Isogen II (Nippon Gene) and the First-Strand cDNA Synthesis Kit (GE Healthcare) and was inserted into the pENTR/D-TOPO vector using the pENTR/D-TOPO Cloning Kit (Invitrogen). After transfer of this cDNA into the pcDNA3.1-EGFP vector (Addgene), RH7777 or HEK293F cells were transfected with the human CAT1-green fluorescent protein (GFP) vector using Lipofectamine 2000 or 293fectin (Invitrogen), respectively. Cells were selected using G418 (400 $\mu\text{g}/\text{mL}$, Nacalai Tesque), followed by sorting using a JSAN cell sorter (Bay Bioscience) based on GFP expression. For immunization, rats were injected with the transfectants (3×10^7) three times into the subcutis, peritoneal cavity, or tail vein every 2 weeks. Three days after the final administration, spleen cells were fused with P3U1 cells with polyethylene glycol (MW = 4000, Roche). Thereafter, the cells were cultured in hypoxanthine, aminopterin, and thymidine (HAT supplement, Invitrogen)-containing RD medium. For the selection of hybridomas, FCM was used.¹²⁻¹⁵ For the first screening, HEK293F cells stably expressing CAT1-GFP were reacted with the culture supernatant of hybridoma cells for 45 minutes, followed by the incubation with PE-labeled donkey anti-rat IgG pAb (1:200; Jackson ImmunoResearch) for 30 minutes. For the second screening, reactivity of antibodies with HT29 cells (1.5×10^4) transfected with CAT1 or control siRNA (28.8 pmol; Dharmacon) was examined. Three days later, the cells were reacted with anti-CAT1 mAbs or control mAb (10 $\mu\text{g}/\text{mL}$) for 45 minutes, followed by staining with PE-labeled donkey anti-rat IgG pAb for 30 minutes. For the acquisition of mAbs, selected hybridoma clones (1×10^7) were administered to pristine (Sigma-Aldrich)-treated nude mice. Anti-CAT1 mAbs were purified from ascites fluid using Protein G Sepharose (GE Healthcare). A rapid mAb isotyping test kit was used to determine the isotype of the mAbs (Antagen Pharma, Inc).

2.12 | Immunohistochemistry (IHC)

Frozen sections (5 μm) from human colorectal tissues were fixed with 4% paraformaldehyde (PFA, Wako Pure Chemical Industries) for 15 minutes and treated with Block Ace (DS Pharma Biomedical Co., Ltd.) for 30 minutes. Sections were incubated with CA2 mAb (5 $\mu\text{g}/\text{mL}$) at 24°C for 1 hour and reacted with 0.3% H_2O_2 in methanol for 10 minutes. They were reacted with biotinylated rabbit

anti-rat IgG pAb (1:200; Vector Laboratories, Inc) for 1 hour, followed by incubation with avidin-biotinylated enzyme Complex solution (Vector Laboratories) for 30 minutes. Isotype-matched rat IgG ($\gamma 2\text{b}/\kappa$) was used as the control. Immunoreactivity was visualized using 0.05% 3,3'-diaminobenzidine (Dojin Chemicals) and 0.01% H_2O_2 in 0.1 M Tris-HCl (pH 7.4), and sections were counterstained with hematoxylin. IHC scores for CAT1 expression were set based on the standard HER2 test. IHC gave a score of 0-3, indicating the amount of CAT1 in tissue samples. CAT1 expression in normal (adjacent to or distant from CRC) and cancer tissues was estimated as score 0 (negative), score 1 (weak or borderline), score 2 (intermediate), or score 3 (strong) by two pathologists.

2.13 | Internalization activity

For microscopic study, CAT1-GFP-overexpressing HEK293F cells were reacted with anti-CAT1 mAbs (10 $\mu\text{g}/\text{mL}$) at 37°C for 1 hour. Then, cells were fixed with 4% PFA and stained with 4',6-diamidino-2-phenylindole (DAPI, 0.5 $\mu\text{g}/\text{mL}$). Confocal fluorescence images were acquired using FV10C-O (Olympus). For FCM, HCT116 and HT29 cells (1×10^5) were suspended in 100 μL of RD medium with or without anti-CAT1 mAbs (10 $\mu\text{g}/\text{mL}$), and incubated for 1 hour at 37 or 4°C. The cells were mixed with PE-conjugated secondary pAb in 1% BSA-PBS for 30 minutes on ice, followed by FCM analysis.

2.14 | Antibody-dependent cellular cytotoxicity (ADCC)

Human mononuclear cells (PromoCell) were used as effector cells. The ADCC assay was evaluated using CytoTox 96 Non-Radioactive Cytotoxicity Assay Kit (Promega) according to the manufacturer's instructions. Briefly, HT29 cells (1×10^4) as the target were harvested into a 96-well U-bottom plate and then reacted with anti-CAT1 mAbs for 15 minutes at 4°C. After the addition of effector cells, the plate was incubated at 37°C for 4 hours. Subsequently, lactate dehydrogenase release in the supernatants was measured by absorbance at 490 nm using a microplate reader.

2.15 | Migration inhibition assays

Migration assays were performed using modified Boyden chambers with 8- μm pore (BD Falcon). The lower chambers were filled with RD medium containing 0.1% BSA, vitronectin (VN, Chemicon, 10 $\mu\text{g}/\text{mL}$) and neuregulin 1 (NRG-1, Abnova, 10 ng/mL). LS-LM4 (2×10^5 cells) was suspended in 100 μL of 0.1% BSA-RD medium and seeded into upper chambers. To examine the effects of anti-CAT1 mAb (CA2), cells were treated with CA2 or control rat mAb (anti-mouse CD98hc) for 30 minutes at 4°C before seeding. After incubation for 20 hours, migrated cells on the lower surfaces of the filter were fixed and

stained with hematoxylin and counted after wiping off nonmigratory cells remaining on the upper surfaces. Details were described in the previous report.¹¹

2.16 | Analysis of maximum mAb binding and mAb avidity

The avidity of mAbs against CRC cells was evaluated according to our previous report.¹⁶ Briefly, cells were reacted with a range of mAb concentrations (100 ng ~ 30 µg/mL), followed by the incubation with PE-conjugated secondary pAb. The subtracted (Δ) MFI was calculated from MFI with or without primary mAbs, and the maximum mAb binding was estimated. Subsequently, the Δ MFI was plotted against mAb concentration. The avidity constant K_A (M^{-1}) was calculated by the Scatchard plot analysis.

2.17 | In vivo antitumor activity

CRC cells (5×10^5) were implanted subcutaneously into four male KSN nude mice in each group. The day when tumor was first palpable was defined as day 0. The CA2 mAb or isotype control IgG

(100 µg/mouse) was administered intraperitoneally on days 0 and 7. Tumor size was periodically measured and the volume (mm^3) was calculated using the formula $0.5 \times (\text{length}) \times (\text{width})^2$.

2.18 | Statistical analyses

Data were analyzed by one- or two-way repeated measures analysis of variance (ANOVA) followed by Tukey's multiple comparisons test. Statistical analysis was carried out using Prism 7 for Windows (GraphPad). The criterion for significance was * $P < .05$, ** $P < .01$, *** $P < .001$. In prognostic analyses with Kaplan-Meier plots, P values were determined with log-rank test. P -values of the metastasis frequency analysis were determined with Fisher's exact test.

3 | RESULTS

3.1 | SLC7A1/CAT1 as a promising anticancer target

To investigate the DNA copy number alterations in a series of 100 primary CRCs, we used BAC arrays covering the entire human genome. We found genomic changes in all 100 primary CRCs and arranged the

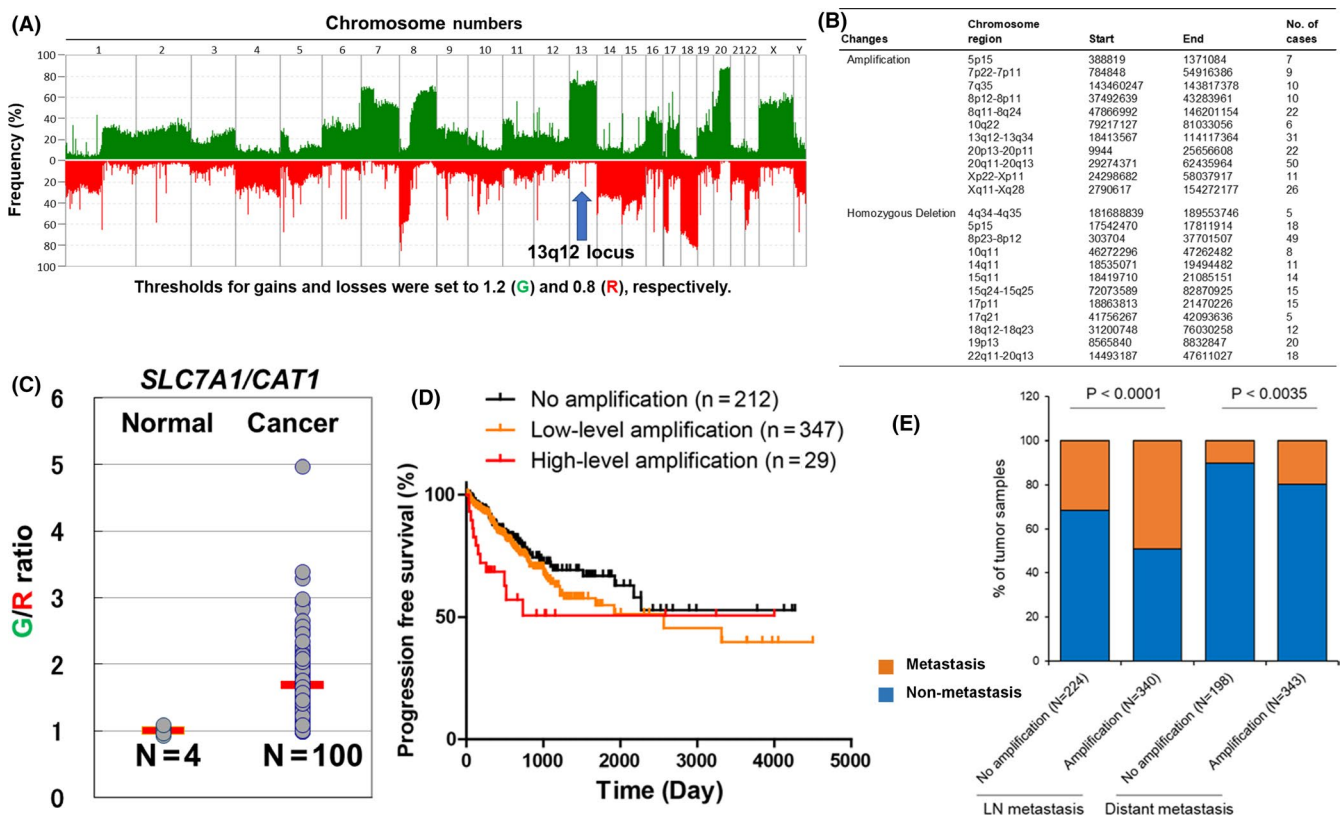


FIGURE 1 Amplifications and homozygous deletions in colorectal cancer (CRC) and correlation between SLC7A1 gene amplification and prognosis and metastasis. A, Green-colored area indicates an increased genome copy number ($G/R > 1.2$), and red-colored area indicates a reduced genome copy number ($G/R < 0.8$). One hundred samples were analyzed. B, High-level amplification and homozygous deletion in CRCs. C, Frequent gene amplification of SLC7A1 located on 13q12. D and E, Correlation between progression-free survival (D), and lymph node and distant metastasis (liver, etc.) (E) of CRC patients and amplification of SLC7A1/CAT1 gene. Data were obtained from The Cancer Genome Atlas (Data set ID: TCGA. COADREAD. SampleMap/Gistic2_CopyNumber_Gistic2_all_data_by_genes)

frequency of gain/loss in CRCs (Figure 1A). Green color indicates an increased genome copy number, and red color represents a reduced genome copy number. Thresholds for gains and losses were set to 1.2 and 0.8, respectively. The most frequent genomic aberrations were gains of chromosome 7, 8q, 13, 20, and X, which occurred at high frequencies (>40%) in CRC tumors. A high level of amplification was observed at seven chromosome regions, including 5p15, 7p22-7p11, 7q35, 8p12-8p11, 8q11-8q24, 10q22, 13q12-13q34, 20p13-20p11, 20q11-20q13, Xp22-Xp11, and Xq11-Xq28 (Figure 1B). Five chromosomes 8p, 15, 17p, 18, and 22p had losses at a high frequency (>40%). High-level homozygous deletions were detected in 4q34-4q35, 5p15, 8p23-8p12, 10q11, 14q11, 15q11, 15q24-15q25, 17q11, 17q21, 18q12-18q23, 19p13, and 22q11-22q13 (Figure 1B).

We next examined the expression levels of regions associated with genomic amplification. Gene expression levels were found to be highly dependent on gene copy number. Our genomic DNA microarray made with complete coverage of the human genome included 23 105 genes. To obtain further information on genes encoding transmembrane proteins, we searched their functional characteristics using the NCBI database. We found 4063 genes encoding transmembrane proteins as possible candidates for anticancer treatment using mAbs. On the basis of analysis of high-level amplifications, we found 16 genes encoding transmembrane proteins at the 13q12 locus (Figure 1A), which includes more than 90 genes. Of note, the *SLC7A1/CAT1* gene was overexpressed in more than 70% of CRCs compared with normal tissues (Figure 1C).

Progression-free survival of CRC patients with high-level amplification was decreased ($P = .0092$) as compared with patients with no amplification of the *SLC7A1/CAT1* gene (Figure 1D) from The Cancer

Genome Atlas (TCGA) cohort. In addition, positive correlation between *CAT1* amplification and CRC metastasis analyzed by TCGA database was shown (Figure 1E).

CAT1 mRNA was also highly expressed (Figure 2A) in the 16 genes of 13q12 locus. Gene amplification and mRNA expression of *SLC7A1/CAT1* were well correlated (Figure 2B). To investigate the function of the *CAT1* gene in CRC cells, we specifically silenced the *CAT1* gene using siRNA. Transfection of HCT116 and LS1034 human colon cancer cells with *CAT1* siRNAs resulted in ~ 10% (HCT116) and ~ 33% (LS1034) of the mRNA level of control cultures (Figure 2C). Four days after siRNA transfections into HCT116 and LS1034 cells, *CAT1* silencing reduced the number of viable cells to 70% of the control (Figure 2D).

3.2 | Production of antihuman *CAT1* mAbs

Antibodies secreted from hybridomas were screened for reactivity against HEK293F cells stably expressing GFP-*CAT1* in a GFP expression level-dependent manner, and five hybridoma clones were selected (Figure 3A). We designated mAbs secreted from these clones as CA1 ~ CA5, and their isotype was IgG ($\gamma 2b/\kappa$). Next, to confirm that anti-*CAT1* mAbs reacted specifically with human *CAT1* protein, we analyzed the influence of *CAT1* siRNA on the reactivity of mAbs in HT29 CRC cells. FCM analysis revealed that treatment with the siRNA remarkably reduced the reactivity of all five anti-*CAT1* mAbs with HT29 cells (Figure 3B). Taken together, our novel mAbs (CA1 ~ CA5) are specific to human *CAT1* proteins.

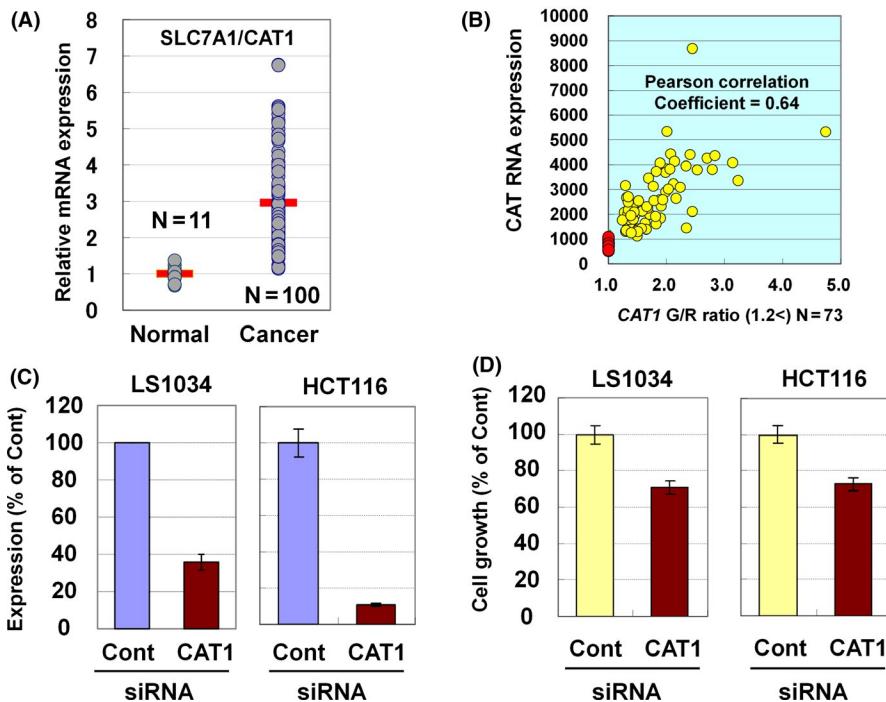


FIGURE 2 Correlation between gene amplification and mRNA expression of *SLC7A1/CAT1* and *CAT1* small interfering RNA (siRNA)-mediated growth inhibition of colorectal cancer (CRC) cells. A, Relative mRNA expression (ratio from a mean value of normal tissues) in normal and cancer tissues. B, Correlation between gene amplification and mRNA expression of *SLC7A1*. C, *CAT1* mRNA levels in HCT116 and LS1034 cells treated with *CAT1* siRNA for 24 hours. D, CRC cell growth 48 hours after treatment with *CAT1* siRNA

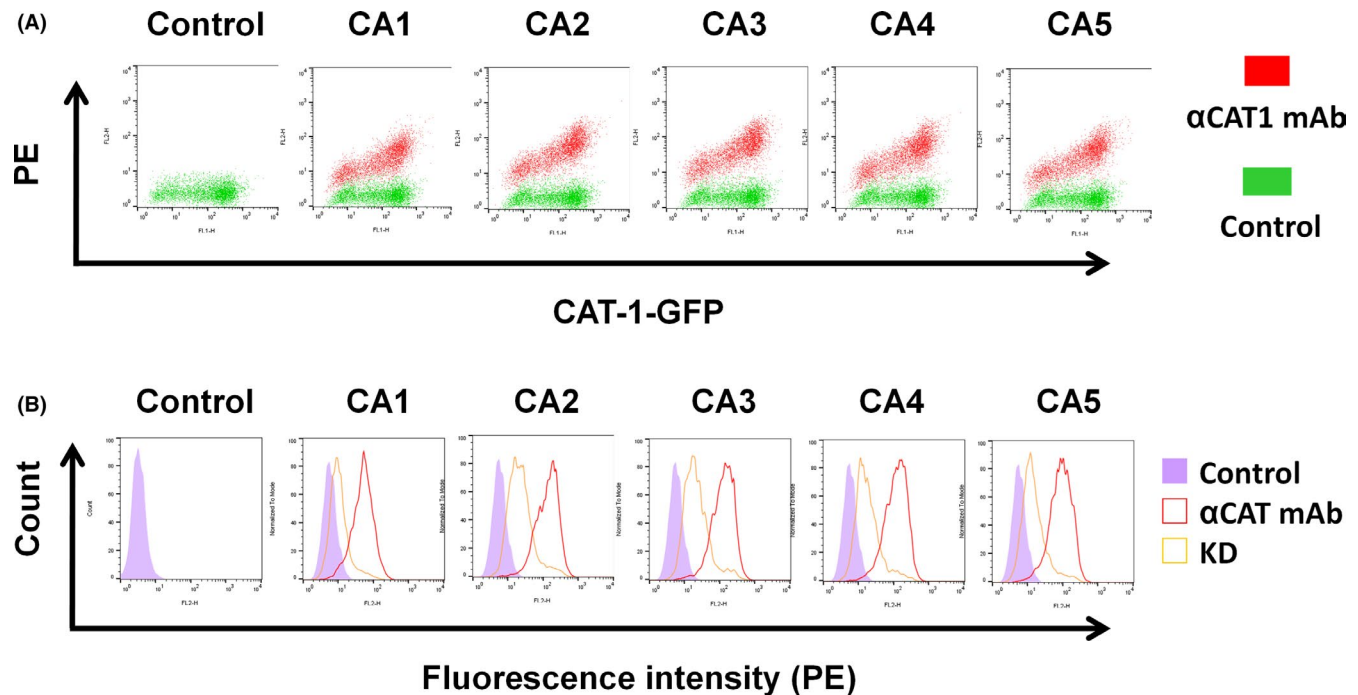


FIGURE 3 Specificity of anti-human CAT1 monoclonal antibodies (mAbs) demonstrated by flow cytometry (FCM). A, Representative FCM dot plot of HEK293F cells expressing CAT1-green fluorescent protein (GFP) stained with anti-CAT1 mAbs. B, Representative FCM histograms of anti-CAT1 mAb-stained HT29 cells, which were treated with CAT1 small interfering RNA (siRNA) (orange lines) or control siRNA (red lines) for 72 h

3.3 | Reactivity of anti-CAT1 mAbs with human colorectal tissues

IHC revealed that the protein expression level of CAT1 in cancerous tissues is higher than that in noncancerous tissues (Figure 4A). For example, the IHC score was 3 in cancer (No 3 ca) and 1 (No 3 nor) in a colon specimen. In 13 cases, for which the clinical information is shown in Figure 4B, the positive ratio of anti-CAT1 (CA2) mAb against CRCs was 100% (13/13: scores 1, 2, and 3) or 69% (9/13: scores 2 and 3). In a low-CGH (1.1) sample (No 7 ca), CAT1 proteins were detected by the CA2 anti-CAT1 mAb, as in high-CGH (2.0 ~ 2.4) samples (No 1 ~ 4 ca).

3.4 | Reactivity of anti-CAT1 mAbs against human CRC cell lines

As shown in Figure 5A, we found that all five CA1 ~ CA5 anti-CAT1 mAbs were strongly reactive against four typical human CRC cell lines, and CA2 exhibited the highest reactivity. Thus, we used CA2 to analyze CAT1 protein expression in additional human cancer cell lines. FCM analysis revealed that CAT1 proteins were highly expressed on the surface of all 16 CRC cell lines examined in this study (Figure 5B). SW1116 and its clone (SW-C4) was indistinguishable in CAT1 expression, and a highly liver-metastatic clone (LS-LM4) showed higher expression of CAT1 as compared with parental LS174T. Furthermore, CA2 reacted with four pancreatic, two breast, and two lung human cancer cell lines (Figure 5C).

3.5 | Internalization, ADCC, and migration inhibition by anti-CAT1 mAbs

Internalization of target molecules and ADCC activity are known as the main mechanisms of *in vivo* antitumor activity of therapeutic mAbs. We examined whether anti-CAT1 mAbs internalize CAT1 proteins and induce ADCC. Fluorescence images of HEK293 cells stably expressing GFP-fused human CAT1 proteins are shown in Figure 6A. Green fluorescence was observed in the membrane of control mAb-treated cells. However, in anti-CAT1 mAb (CA3)-treated cells, intracellular punctate or granular staining was observed. The remaining four mAbs also caused the internalization of CAT1 proteins (data not shown). Quantification of CAT1 surface expression levels in anti-CAT1 mAb-treated HCT116 (Figure 6B) and HT29 (Figure 6C) cells by FCM was shown. MFI demonstrating cell surface CAT1 expression was reduced after incubation at 37°C (red-colored bars) compared with after that at 4°C (blue-colored bars). The ADCC activity of five anti-CAT1 mAbs against HT29 cells is shown in Figure 6D, and CA2 and CA3 had higher ADCC activity than the other mAbs. The effector/target ratio- and mAb concentration-dependent ADCC activity of CA2 and CA3 against HT29 cells are shown in Figure 6E,F, respectively. Furthermore, anti-CAT1 mAb (10 μ g/mL) almost completely inhibited NRG-1-induced migration of highly liver-metastatic colon cancer cells, LS-LM4, although control (anti-mouse CD98 mAb) did not inhibit the migration (Figure 6G).

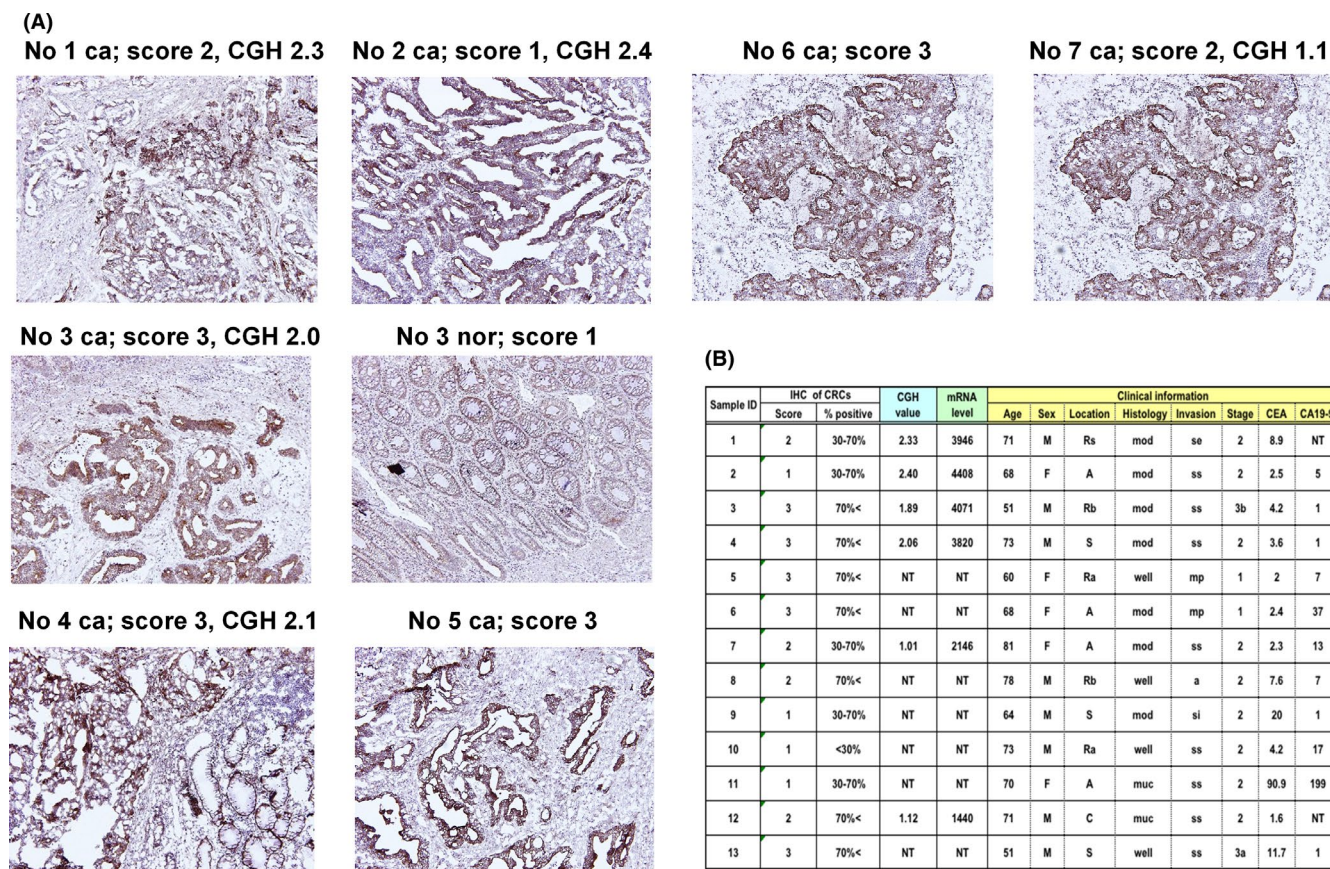


FIGURE 4 Immunostaining of human colorectal tissues by anti-CAT1 monoclonal antibody (mAb) and patient information. A, Representative staining of human colorectal cancer (CRC) tissues (sample 3 was paired with normal colon) by CA2. Immunoscoring (1-3) and comparative genomic hybridization (CGH) values are shown. B, Clinical information of CRC patients is summarized. Patient sex: M, male; F, female. Tumor location: A, ascending colon; S, sigmoid colon; Rs, rectosigmoid; Ra, upper rectum; Rb, lower rectum; C, cecum. Tumor histology: mod, moderately differentiated adenocarcinoma; well, well-differentiated adenocarcinoma; muc, mucinous adenocarcinoma

3.6 | Comparative analysis with mAbs against AA transporters and antitumor effects of anti-CAT1 mAbs

Lastly, we investigated whether our novel anti-CAT1 mAbs inhibit CRC tumor growth. Prior to this experiment, we compared the reactivity of CA2 against CRC cells with mAbs recognizing other tumor-associated AA transporters (LAT1 and xCT). Scatchard analysis revealed a two-mode pattern of binding, which matches dual (high and low) avidities. High mode is represented by approximately 3%-11% of total binding with avidity $K_A > 10^8 \text{ M}^{-1}$. Low mode represents binding with avidity $K_A > 10^6 \text{ M}^{-1}$ and constitutes approximately 89%-96% of the total mAb binding (Figure 7A and 7B). However, CA2 demonstrated superior maximum binding against HT29 and SW-C4 CRC cells compared with mAbs against LAT1 or xCT (Figure 7A and 7B). The antitumor effects of mAbs on CRC cells in a xenograft model are shown in Figure 7(C and D), and CA2 significantly inhibited the tumor growth of HT29 and SW-C4 cells compared with control IgG.

4 | DISCUSSION

We recently surveyed gain or loss genomic aberration in CRCs. Loss of chromosome 18, and gains of chromosome 13 and 20,

which were detected in this study, are most common in CRCs, as confirmed in previous studies.^{17,18} In addition, other recurrent losses and gains of whole chromosomes were found; namely, losses on 1p, 4, 14, 15, 21, and 22q, and gains on 1q, 2, 3q, 5p, 6, 9, 11, 12, 16, 17q, and 19. The rates of some of these alterations are consistent with previous reports.¹⁹⁻²² Loss of chromosome 1p and gain of chromosome 1q are major events to form an isochromosome; however, the formation of isochromosome in CRC is unknown.^{19,22} Based on the analysis of high-level gene amplifications, *SLC7A1/CAT1* was identified as a gene overexpressed in approximately 70% of CRCs compared with normal colon tissues, and a higher level of CAT1 mRNA was also demonstrated by RT-qPCR analysis.

SLC7A1 encodes a cationic AA transporter 1 (CAT1) that has 14 putative transmembrane domains,^{23,24} and is responsible for the uptake of cationic AAs (arginine, lysine, and ornithine). Although CAT/SLC7A1~4 are primary transporters for arginine uptake, CAT1 is the highest-affinity transporter for arginine among the CAT family.²⁵ There are several reports of the overexpression of CAT1 mRNA and protein in different cancers such as breast cancer and CRCs.²⁶⁻²⁸ However, it is unclear whether CAT1 is a therapeutic target for human cancers.

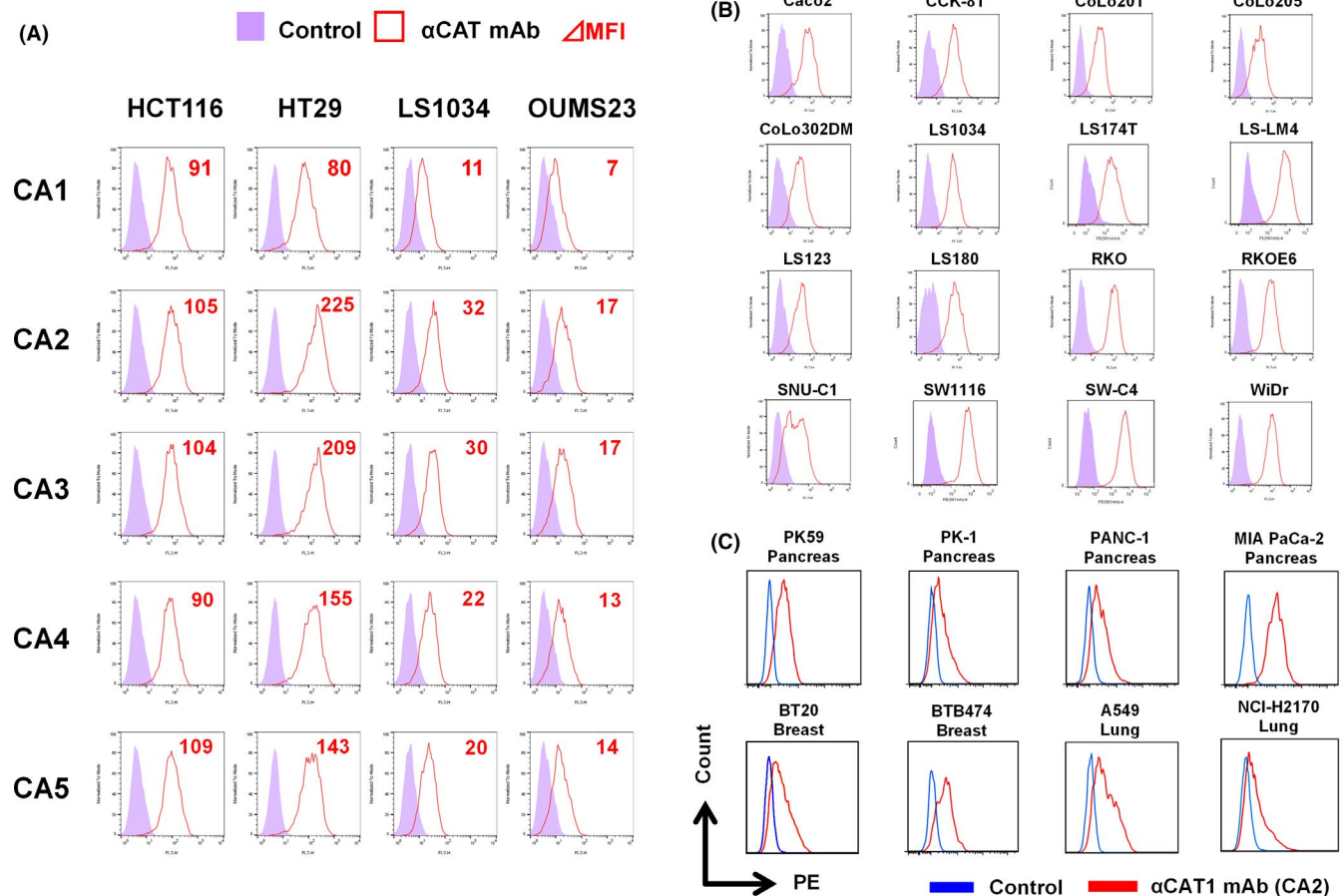


FIGURE 5 Specificity of anti-CAT1 monoclonal antibodies (mAbs) against human cancer cell lines. A, Representative flow cytometry (FCM) histograms of human colorectal cancer (CRC) cell lines stained with anti-CAT1 mAbs. B and C, Different human CRC cell lines (B), and pancreatic, breast, and lung cancer cell lines (C) were reacted with CA2 or isotype-matched control mAb, followed by incubation with phycoerythrin (PE)-labeled anti-rat IgG polyclonal antibody (pAb). The fluorescence intensity of individual cells was measured by FCM

We demonstrated that siRNA-mediated KD of CAT1 results in the growth inhibition of HCT116 and LS1034 cells, suggesting an essential role of CAT1 in the growth of CRC cells. Furthermore, we produced novel anti-human CAT1 mAbs and found that they suppressed in vivo tumor growth of CRC cells in nude mice. As possible anti-tumor mechanisms, the reduction of cell-surface CAT1 expression by internalization activity and induction of ADCC was confirmed in this study, suggesting that CAT1 is a suitable anticancer therapeutic target.

CRC is regarded as a considerable health issue worldwide because of the high death rate²⁹ and prediction of increased incidence.³⁰ As a feature of CRC, genetic alterations, including *KRAS*, *PIK3CA*, *BRAF*, and *TP53*, are common and are the driving force of carcinogenesis.³¹ Although cetuximab and panitumumab are used to treat CRCs, both mAbs are less effective against tumors harboring these genetic mutations.^{32–34} Our present study revealed that CAT1 was overexpressed in more than 69% (IHC score > 2:9/13) or 80% (CGH > 2.0:4/5) of CRCs. From TCGA database, amplification of *SLC7A1/CAT1* gene seems a poor prognostic factor, because progression-free survival of CRC patients with high-level amplification was significantly decreased as compared with

patients with no amplification of *SLC7A1/CAT1* gene. Trastuzumab is a clinically successful drug, targeting the receptor-type tyrosine kinase HER2,^{8,35} which is overexpressed in only 20 ~ 30% of breast cancers. Taking the “oncogene addiction”-based efficacy of trastuzumab into consideration, CAT1 may be a potential target for mAb therapy of CRCs based on “oncogenic AA transporter addiction.” Furthermore, we found that the CA2 mAb suppressed tumor growth of HT29 and SW-C4 cells, which harbor *BRAF* and *PIK3CA*, and *KRAS* and *TP53*, respectively.³⁶ This suggests that CAT1-targeted therapy is powerful, independently of various genetic mutations.

In both lymph node and distant (liver, etc.) metastases from TCGA data, frequency was significantly high in patients with gene amplification, as compared with patients with no amplification of *SLC7A1/CAT1*. As to preferential metastasis of CRC to the liver, anti-CAT1 mAb therapy may be useful because a highly liver-metastatic CRC cell clone showed higher expression of CAT1 as compared with a parental cell line. Furthermore, migration of highly liver-metastatic CRC cells was significantly inhibited by anti-CAT1 mAb, suggesting possible therapeutic effects of anti-CAT1 mAb on the metastatic process of CRCs.

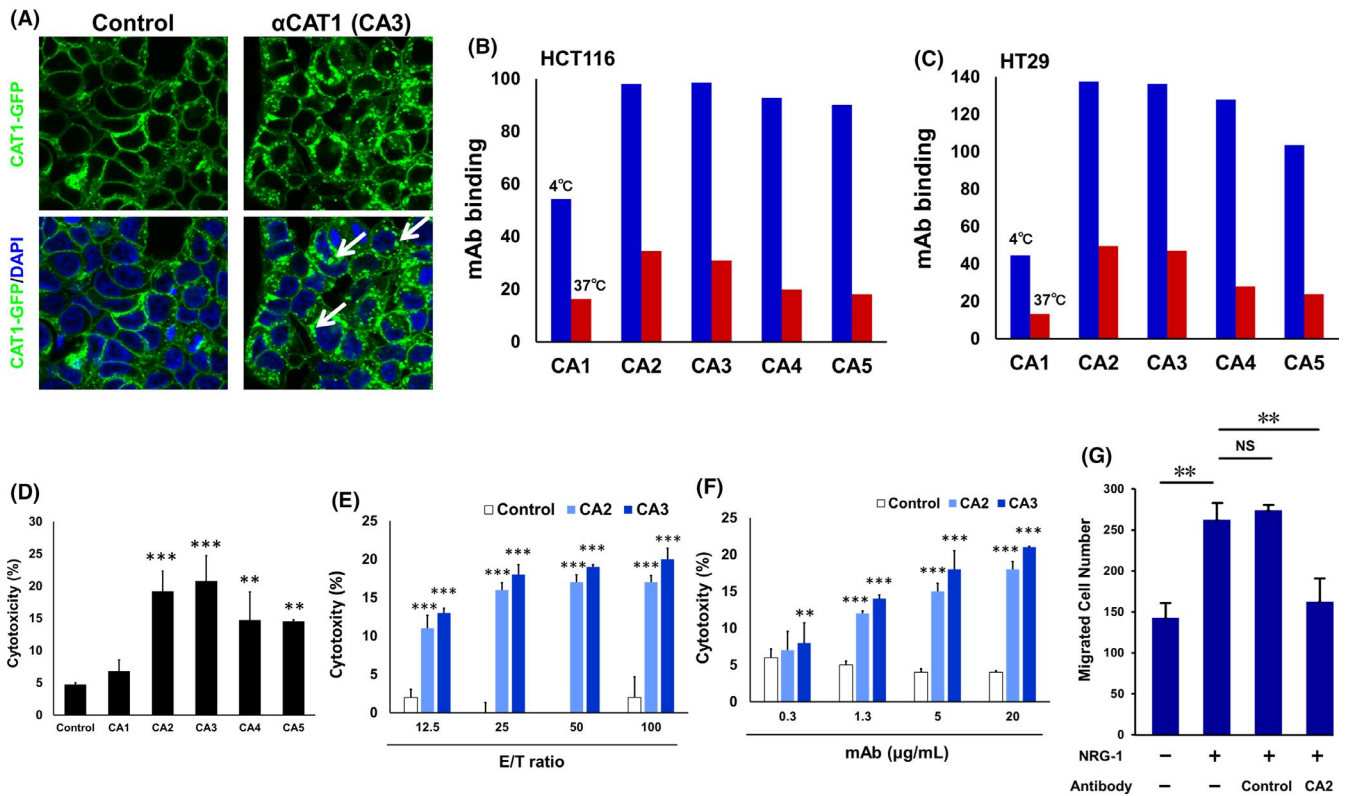


FIGURE 6 Internalization, antibody-dependent cellular cytotoxicity (ADCC), and migration inhibition assays by anti-CAT1 monoclonal antibodies (mAbs). A, Representative images of anti-CAT1 mAb-treated HEK293F cells expressing CAT1-green fluorescent protein (GFP) proteins. Nuclei were stained with DAPI. B and C, Quantitative analysis of internalization by flow cytometry (FCM). Subtracted mean fluorescence intensity (Δ MFI) was calculated based on the MFI with or without primary mAbs, and indicated as mAb binding. D-F, ADCC activity was measured by lactate dehydrogenase release assay. D, ADCC assay at an effector/target (E/T) ratio of 50 and 20 μ g/mL with CA1 ~ CA5 mAbs. E, E/T ratio-dependent assay at 20 μ g/mL with CA2 and CA3 mAbs. F, mAb concentration-dependent assay at an E/T ratio of 50 with CA2 and CA3 mAbs. G, Abrogation of NRG-1-induced vitronectin (VN)-mediated migration of highly liver-metastatic LS-LM4 cells by anti-CAT1 mAb. VN-mediated migration of LS-LM4 cells, enhanced by NRG-1 (10 ng/mL) is abolished by 10 μ g/mL of CA2 anti-CAT1 mAb (** $P < .0035$, two-way ANOVA)

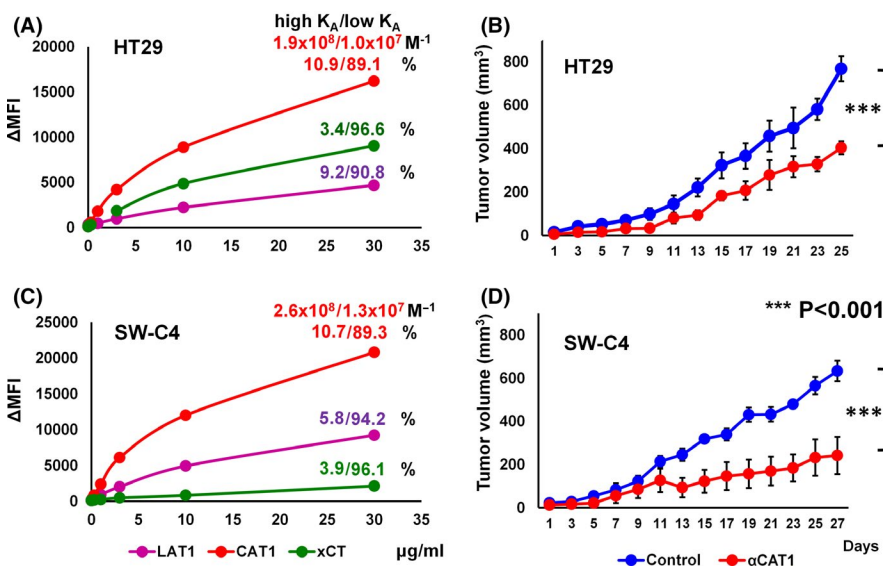


FIGURE 7 Comparative analysis with monoclonal antibodies (mAbs) against amino acid (AA) transporters and in vivo antitumor effects of anti-CAT1 mAb. A and B, Reactivity of mAbs against CAT1, LAT1, or xCT AA transporter was compared. Maximum binding and K_A of mAbs against HT29 and SW-C4 cells was measured by Scatchard plot analysis. C and D, Tumor growth of grafted HT29 or SW-C4 cells in nude mice. On days 0 and 7, CA2 mAb or isotype control IgG ($\gamma 2a/\kappa$) (100 μ g/mouse) was administered intraperitoneally. Data are presented as the mean \pm SEM ($n = 4$). Δ MFI, subtracted mean fluorescence intensity

Although arginine is classified as a nonessential AA in normal cells, several kinds of tumors are auxotrophic for this AA due to the loss or downregulation of argininosuccinate synthetase,^{37,38}

which catalyzes the conversion of citrulline to arginine. Therefore, survival and proliferation of these kinds of tumors depend on extracellular arginine transport into cells. Arginine plays an essential

role in the synthesis of biological molecules, and nitric oxide (NO) is one such molecule. NO has protumorigenic effects such as increased cell proliferation, angiogenesis induction, and resistance to apoptosis.^{39,40} There are several reports that arginine-depleting agents targeting arginine-lowering enzymes (arginine deiminase and arginase I) induce the inhibition of cell viability and apoptosis in vitro, and suppression of tumor growth in vivo in a variety of cancers.⁴¹ Therefore, targeting arginine may be efficacious for cancer treatment.

Glutamine is an important nutrient for many cancers, and suppression of its supply is considered a novel strategy for cancer therapy. However, glutamine deprivation was followed by increased intracellular arginine levels via the upregulation of SLC7A3.³⁹ On the other hand, arginine deprivation induced increased glutamine anaplerosis.⁴² Taken together, these findings suggest that inhibition of the transport of only a single AA is not sufficient to treat cancer. We developed novel mAbs against ASCT2⁴³ and LAT1,¹⁶ which transport glutamine and branched-chain AAs, respectively. Following our recent discovery of dual avidity status in the binding of anti-LAT1 mAb,¹⁶ anti-CAT1 mAb also exhibited high and low avidity modes against CRC cells. We consider simultaneous inhibition of multiple AA transporters, such as CAT1, ASCT2, and LAT1, to be a more efficient therapeutic strategy. Further studies are required to conclude the efficacy of such combination therapy. In the present study, we successfully developed novel anti-human CAT1 mAbs, which inhibited CRC-derived tumor growth possibly through the internalization of CAT1 and induction of ADCC. Recently, attention has been paid to therapy for different cancers targeting arginine depletion by enzymatic degradation. Our present study supports the efficacy of targeting arginine as a therapeutic strategy and suggests CAT1 as a novel target for cancer therapy.

ACKNOWLEDGMENTS

This study was supported by the MEXT-Supported Program for the Strategic Research Foundation at Private Universities, 2014–2018 (S1411037 to Sugiura R) and by Grant-in-Aid for Scientific Research from the Japan Society for the Promotion of Science (JSPS, KAKENHI), 2016–2020 (16K10476 to Sakamoto K). The corresponding author (TM) is deeply grateful to Dr Hamada Y (HAMADA NAIKA CLINIC) for his careful examination and to Dr Yamamoto K (Osaka Hospital, Japan) for the complete endoscopic submucosal dissection of a colon tumor of TM, which was detected in the process of this manuscript preparation.

CONFLICT OF INTEREST

The authors have no conflict of interest to declare.

ORCID

Reiko Sugiura  <https://orcid.org/0000-0001-6946-0935>

Hiromitsu Komiyama  <https://orcid.org/0000-0003-4298-3829>

Takashi Masuko  <https://orcid.org/0000-0002-2410-2007>

REFERENCES

1. Fearon ER, Vogelstein B. A genetic model for colorectal tumorigenesis. *Cell*. 1990;61:759-767.
2. Sato T, Tanigami A, Yamakawa K, et al. Allelotype of breast cancer cumulative allele losses promote tumor progression in primary breast cancer. *Cancer Res*. 1990;50:7184-7189.
3. Barnekow A, Paul E, Scharf M. Expression of the c-src protooncogene in human skin tumors. *Cancer Res*. 1987;47:235-240.
4. Weinstein IB. Disorders in cell circuitry during multistage carcinogenesis: the role of homeostasis. *Carcinogenesis*. 2000;21:857-864.
5. Cancer WIB. Addiction to oncogenes—the Achilles heel of cancer. *Science*. 2002;297:63-64.
6. Lynch TJ, Bell DW, Sordella R, et al. Activating mutations in the epidermal growth factor receptor underlying responsiveness of non-small-cell lung cancer to gefitinib. *N Engl J Med*. 2004;350:2129-2139.
7. Shepherd FA, Rodrigues Pereira J, Ciuleanu T, et al. Erlotinib in previously treated non-small-cell lung cancer. *N Engl J Med*. 2005;353:123-132.
8. Slamon DJ, Leyland-Jones B, Shak S, et al. Use of chemotherapy plus a monoclonal antibody against HER2 for metastatic breast cancer that overexpresses HER2. *N Engl J Med*. 2001;344:783-792.
9. Cunningham D, Humblet Y, Siena S, et al. Cetuximab monotherapy and cetuximab plus irinotecan in irinotecan-refractory metastatic colorectal cancer. *N Engl J Med*. 2004;351:337-345.
10. Weinstein IB, Joe AK. Mechanisms of disease: oncogene addiction—a rationale for molecular targeting in cancer therapy. *Nat Clin Pract Oncol*. 2006;3:448-457.
11. Yoshioka T, Nishikawa Y, Ito R, et al. Significance of integrin $\alpha v \beta 5$ and erbB3 in enhanced cell migration and liver metastasis of colon carcinomas stimulated by hepatocyte-derived heregulin. *Cancer Sci*. 2010;101:2011-2018.
12. Hara Y, Torii R, Ueda S, et al. Inhibition of tumor formation and metastasis by a monoclonal antibody against lymphatic vessel endothelial hyaluronan receptor 1. *Cancer Sci*. 2018;109:3171-3182.
13. Okita K, Okazaki S, Uejima S, et al. Novel functional anti-HER3 monoclonal antibodies with potent anti-cancer effects on human epithelial cancers. *Oncotarget*. 2020;11:31-45.
14. Ohno Y, Suda K, Masuko K, Yagi H, Hashimoto Y, Masuko T. Production and characterization of highly tumor-specific rat monoclonal antibodies recognizing the extracellular domain of human LAT1 amino-acid transporter. *Cancer Sci*. 2008;99:1000-1007.
15. Masuko T, Ohno Y, Masuko K, et al. Towards therapeutic monoclonal antibodies to membrane oncoproteins by a robust strategy using rats immunized with transfectants expressing target molecules fused to green fluorescent protein. *Cancer Sci*. 2011;102:25-35.
16. Ueda S, Hayashi K, Miyamoto T, et al. Anti-tumor effects of mAb against L-type amino-acid transporter 1 (LAT1) bound to human and monkey LAT1 with dual avidity modes. *Cancer Sci*. 2019;110:674-685.
17. Mampaey E, Fieeuw A, Van Laethem T, et al. Focus on 16p13.3 locus in colon cancer. *PLoS One*. 2015;10(7):e0131421.
18. Carvalho B, Postma C, Mongera S, et al. Multiple putative oncogenes at the chromosome 20q amplicon contribute to colorectal adenoma to carcinoma progression. *Gut*. 2009;58:79-89.
19. Diep CB, Kleivi K, Ribeiro FR, Teixeira MR, Lindgjaerde OC, Lothe RA. The order of genetic events associated with colorectal cancer progression inferred from meta-analysis of copy number changes. *Gene Chromosomes Cancer*. 2006;45:31-41.
20. Loo LW, Tiirikainen M, Cheng I, et al. Integrated analysis of genome-wide copy number alterations and gene expression in microsatellite stable, CpG island methylator phenotype-negative colon cancer. *Gene Chromosomes Cancer*. 2013;52:450-466.
21. Sawada T, Yamamoto E, Suzuki H, et al. Association between genomic alterations and metastatic behavior of colorectal cancer

- identified by array-based comparative genomic hybridization. *Gene Chromosomes Cancer*. 2013;52:140-149.
22. Shi ZZ, Zhang YM, Shang L, et al. Genomic profiling of rectal adenoma and carcinoma by array-based comparative genomic hybridization. *BMC Med Genomics*. 2012;5:52.
 23. Verrey F, Closs E, Wagner C, Palacin M, Endou H, Kanai Y. CATs and HATs: the SLC7 family of amino acid transporters. *Pflugers Arch*. 2004;447:532-542.
 24. Mann GE, Yudilevich DL, Sobrevia L. Regulation of amino acid and glucose transporters in endothelial and smooth muscle cells. *Physiol Rev*. 2003;83:183-252.
 25. Closs EI, Simon A, Vékony N, Rotmann A. Plasma membrane transporters for arginine. *J Nutr*. 2004;134:2752S-2759S.
 26. Abdelmagid SA, Rickard JA, McDonald WJ, Thomas LN, Too CK. CAT-1-mediated arginine uptake and regulation of nitric oxide synthases for the survival of human breast cancer cell lines. *J Cell Biochem*. 2011;112:1084-1092.
 27. Vardon A, Dandapani M, Cheng D, Cheng P, De Santo C, Mussai F. Arginine auxotrophic gene signature in paediatric sarcomas and brain tumours provides a viable target for arginine depletion therapies. *Oncotarget*. 2017;8:63506-63517.
 28. Dai R, Peng F, Xiao X, et al. Hepatitis B virus X protein-induced upregulation of CAT-1 stimulates proliferation and inhibits apoptosis in hepatocellular carcinoma cells. *Oncotarget*. 2017;8:60962-60974.
 29. Ferlay J, Soerjomataram I, Dikshit R, et al. Cancer incidence and mortality worldwide: sources, methods and major patterns in GLOBOCAN 2012. *Int J Cancer*. 2015;136:E359-E386.
 30. Arnold M, Sierra MS, Laversanne M, Soerjomataram I, Jemal A, Bray F. Global patterns and trends in colorectal cancer incidence and mortality. *Gut*. 2017;66:683-691.
 31. Markowitz SD, Bertagnolli MM. Molecular origins of cancer: Molecular basis of colorectal cancer. *N Engl J Med*. 2009;361:2449-2460.
 32. Amado RG, Wolf M, Peeters M, et al. Wild-type KRAS is required for panitumumab efficacy in patients with metastatic colorectal cancer. *J Clin Oncol*. 2008;26:1626-1634.
 33. Di Nicolantonio F, Martini M, Molinari F, et al. Wild-type BRAF is required for response to panitumumab or cetuximab in metastatic colorectal cancer. *J Clin Oncol*. 2008;26:5705-5712.
 34. Lièvre A, Bachet JB, Boige V, et al. KRAS mutations as an independent prognostic factor in patients with advanced colorectal cancer treated with cetuximab. *J Clin Oncol*. 2008;26:374-379.
 35. Piccart-Gebhart MJ, Procter M, Leyland-Jones B, et al. Trastuzumab after adjuvant chemotherapy in HER2-positive breast cancer. *N Engl J Med*. 2005;353:1659-1672.
 36. Ahmed D, Eide PW, Eilertsen IA, et al. Epigenetic and genetic features of 24 colon cancer cell lines. *Oncogenesis*. 2013;2:e71.
 37. Dillon BJ, Prieto VG, Curley SA, et al. Incidence and distribution of argininosuccinate synthetase deficiency in human cancers: a method for identifying cancers sensitive to arginine deprivation. *Cancer*. 2004;100:826-833.
 38. Miraki-Moud F, Ghazaly E, Ariza-McNaughton L, et al. Arginine deprivation using pegylated arginine deiminase has activity against primary acute myeloid leukemia cells in vivo. *Blood*. 2015;125:4060-4068.
 39. Gerner EW, Meyskens FL Jr. Polyamines and cancer: old molecules, new understanding. *Nat Rev Cancer*. 2004;4:781-792.
 40. Fung MKL, Chan GCF. Drug-induced amino acid deprivation as strategy for cancer therapy. *J Hematol Oncol*. 2017;10:144.
 41. Lowman XH, Hanse EA, Yang Y, Ishak Gabra MB, Tran TQ, Li H. p53 promotes cancer cell adaptation to glutamine deprivation by upregulating Slc7a3 to increase arginine uptake. *Cell Rep*. 2019;26:3051-3060.e4.
 42. Kremer JC, Prudner BC, Lange SES, et al. Arginine deprivation inhibits the warburg effect and upregulates glutamine anaplerosis and serine biosynthesis in ASS1-deficient cancers. *Cell Rep*. 2017;18:991-1004.
 43. Hara Y, Minami Y, Yoshimoto S, et al. Anti-tumor effects of an antagonistic mAb against the ASCT2 amino acid transporter on KRAS-mutated colorectal cancer cells. *Cancer Med*. 2020;9:302-312.

How to cite this article: Okita K, Hara Y, Okura H, et al. Antitumor effects of novel mAbs against cationic amino acid transporter 1 (CAT1) on human CRC with amplified *CAT1* gene. *Cancer Sci*. 2021;112:563-574. <https://doi.org/10.1111/cas.14741>